Journal of Magnetism and Magnetic Materials 385 (2015) 308–312

Contents lists available at ScienceDirect

Journal of Magnetism and Magnetic Materials

journal homepage: www.elsevier.com/locate/jmmm

Magnetic properties of $MnFe_2O_4$ nano-aggregates dispersed in paraffin wax

B. Aslibeiki [a,*], P. Kameli [b]

[a] Department of Solid State Physics, Faculty of Physics, University of Tabriz, Tabriz 51666-16471, Iran
[b] Department of Physics, Isfahan University of Technology, Isfahan 84156-83111, Iran

ARTICLE INFO

Article history:
Received 16 December 2014
Received in revised form
2 March 2015
Accepted 6 March 2015
Available online 9 March 2015

Keywords:
$MnFe_2O_4$
Surface spins
Superparamagnetic
AC susceptibility
Paraffin wax

ABSTRACT

Manganese ferrite, $MnFe_2O_4$ nanoparticles with average size of ~6.5 nm were synthesized by using a thermal decomposition method. The nanoparticles were aggregated which was confirmed by FESEM and TEM images. The aggregates with a diameter of ~50 nm showed interacting superspin glass (SSG) behavior. The powders were dispersed in the molten paraffin wax by using ultrasonic bath. Samples with different paraffin/ferrite weight ratios of $P/F=$ 0, 1, 5, 10 and 20 were prepared. M–H curves of the samples revealed presence of superparamagnetic state at 300 K. Saturation magnetization (M_s) decreased from 26.6 to 1.3 emu/g by increasing the P/F value from 0 to 20, respectively. Furthermore, the VSM measurements showed a decrease in surface spin disorder of paraffin-embedded nanoparticles in comparison with bare particles. The AC magnetic susceptibility peak temperature, T_p increased from 230 to >300 K with increasing the paraffin content in the samples. The present study showed that by dispersing the particles in a non-magnetic matrix, the blocking temperature could be increased.

1. Introduction

In the past decade, magnetic nanoparticles have been widely investigated because of their potential applications in industry and medicine ranging from microwave absorbance, data recording media and ferro-fluids to drug delivery, magnetic hyperthermia, MRI contrasting, etc. [1–5]. Application of magnetic nanoparticles depends on their coercive field, remanent and saturation magnetization, response to the external AC fields, relaxation times, and anisotropy.

$MnFe_2O_4$ ferrite with spinel structure shows interesting features such as simple preparation methods, high saturation magnetization (M_s~83 emu/g at 300 K), high chemical stability and low Curie temperature (T_c~580 K) among spinel ferrites [6]. The $MnFe_2O_4$ nanoparticles show different properties as compared to corresponding bulk sample. The core of nanoparticles consists of almost regular atomic arrangement and shows bulk-like behavior. On the other hand, the shell has structural deficiencies and broken bands. Structural deficiencies lead to an amorphous atomic arrangement in the surface of nanoparticles.

Magnetic properties of nanoparticles can change by embedding in a non-magnetic polymer. Interaction between polymer molecules and surface atoms of nanoparticles can change the surface anisotropy, total anisotropy energy and consequently the coercivity and remanent magnetization [7,8]. Variation of these parameters can change the other properties of system such as blocking temperature and magnetic state.

Herein, we present the structural and magnetic characterization of ~6.5 nm $MnFe_2O_4$ nanoparticles embedded in paraffin wax. After structural characterizations, we studied the effect of paraffin matrix on magnetic properties of the ferrite samples.

2. Experimental

2.1. Synthesis

$MnFe_2O_4$ nanoparticles were synthesized using a thermal decomposition method described elsewhere [9,10]. In a typical synthesis, manganese nitrate ($Mn(NO_3)_2 \cdot 4H_2O$, Merk, 99%), iron nitrate ($Fe(NO_3)_3 \cdot H_2O$, Merk, 99%), and citric acid ($C_6H_6O_7$, Merk, 99.5%) were mixed together by an equal molar ratio of total metal nitrates to citric acid. The powders were ball milled and then were annealed in ambient air at 350 °C for 1 h. The obtained black powders were $MnFe_2O_4$ nanoparticles. In the next step, the ferrite sample was dispersed in molten paraffin using an ultrasonic bath. Samples with different paraffin/ferrite weight (P/F) ratios of 0, 1, 5, 10 and 20 were prepared. The samples were named as P0, P1, P5, P10 and P20 according to P/F ratio from 0 to 20 respectively.

* Corresponding author. Fax: +98 41 33341244.
E-mail address: b.aslibeiki@tabrizu.ac.ir (B. Aslibeiki).

http://dx.doi.org/10.1016/j.jmmm.2015.03.023
0304-8853/

2.2. Experimental techniques and data treatment

X-ray diffraction (XRD) pattern of the samples was taken on a Philips X′Pert Pro MPD X-ray diffractometer with Cu-Kα radiation (λ=0.154 nm). Fourier transform infrared (FTIR) spectra were recorded using a Tensor 27 spectrometer within the range of 400–3500 cm^{-1}. Nanostructural, morphology and elemental composition of the samples were studied using a transmission electron microscope (TEM) and a Hitachi Model S-4160 field emission scanning electron microscope (FESEM) equipped with energy-dispersive X-ray (EDX) spectroscopy. Magnetic hysteresis curves were recorded by a vibrating sample magnetometer (VSM) with a maximum field of 20 kOe. Dynamic magnetic susceptibility measurements were performed by an AC susceptometer (Lake Shore 7000). The measurements were carried out by cooling the sample from room temperature to 80 K in zero magnetic field and then the magnetic susceptibility was measured during the warming process in a magnetic field of 10 Oe and frequency of 333 Hz.

3. Results and discussion

3.1. Structural properties

Fig. 1a shows Rietveld refinement of XRD data of the P0 sample. In Fig. 1a the red spheres represent experimental data; the black solid line is calculated values by using Rietveld method, and the blue line shows residuals. Results show that the calculated values are in good accordance with experimental data. Furthermore, there is no noticeable trace of secondary phases in the XRD pattern which confirms single spinel phase of the sample. For comparison, the XRD pattern and Rietveld refinement of bulk $MnFe_2O_4$ is presented in Fig. 1b.

Average crystallite size and the lattice constant (a) of the $MnFe_2O_4$ sample were calculated using the following formula:

$$\langle D_{XRD}\rangle = \frac{K\lambda}{\beta\cos\theta} \quad (1)$$

$$\frac{1}{d^2} = \frac{h^2+k^2+l^2}{a^2} \quad (2)$$

In Eq. (1) which is called Debye–Scherrer's formula, β is the full-width at half-maximum (FWHM) of the XRD peaks, θ is the Bragg angle, K is the Scherrer's constant which is a dimensionless factor related to the shape of crystallites, with a value close to unity (~0.9) and λ is the wavelength of the radiation. Eq. (2) in which the (h,k,l) are Miller indexes, is used for the cubic spinel structure. Using Scherrer's formula the average crystallite size $\langle D\rangle$=6.5($\pm$0.5) nm was obtained. The obtained a=8.34($\pm$0.03) Å using Eq. (2) was smaller than that of bulk $MnFe_2O_4$ (8.51 Å) [6]. Oxidation of Mn^{2+} to Mn^{3+} and different cation distributions of ferrite nanoparticles can decrease the lattice constant [11,12]. Cation distribution in bulk Mn-ferrite is demonstrated as $\left(Mn_{0.8}^{2+}Fe_{0.2}^{3+}\right)_A\left(Mn_{0.2}^{2+}Fe_{1.8}^{3+}\right)_B$, where A and B denote the tetrahedral and octahedral sites in spinel structure, respectively. Oxidation of Mn^{2+} (0.81 Å) to Mn^{3+} (0.72 Å) reduces the lattice parameter. Yang et al. obtained a=8.4 Å for ~7.5 nm $MnFe_2O_4$ nanoparticles prepared by a modified co-precipitation method [11]. They justified this result by different cation distribution of nanopartices compared to bulk manganese ferrite. Similar results have been reported in the literature [13–14].

Fig. 2 shows FTIR spectra of the samples. The double peaks at 2919 cm^{-1} and 2850 cm^{-1} are assigned to the C–H symmetrical and asymmetrical stretching bonds. The absorption band at

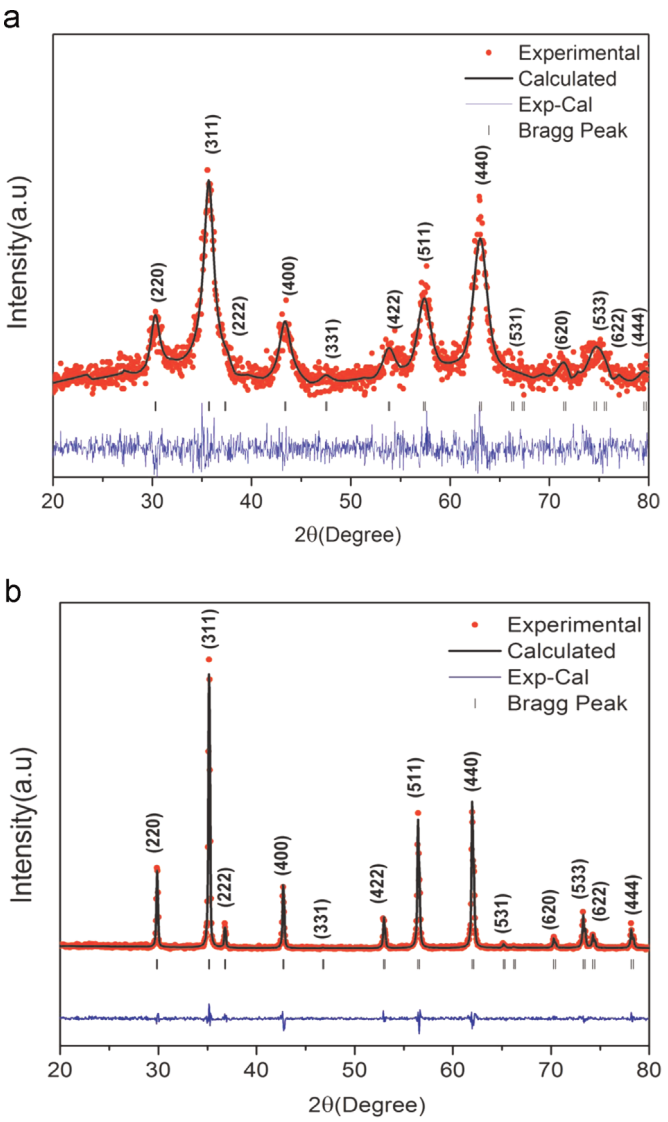

Fig. 1. (a) XRD pattern of $MnFe_2O_4$ nanoparticles. Red spheres are experimental data, and the solid black line represents the Rietveld refinement. The blue line shows the residuals. (b) XRD pattern and Rietveld refinement of bulk $MnFe_2O_4$. (For interpretation of the references to color in this figure legend, the reader is referred to the web version of this article.)

1466 cm^{-1} is attributed to the C–H bending vibration. The peak at 724 cm^{-1} is in-plane rocking vibration of the CH_2 group of paraffin. It is clear from FTIR spectra that, the intensity of C–H groups increases with increasing the paraffin content in the samples. There is a signature of two important bands below 1000 cm^{-1} in FTIR spectra. The peak at 560 cm^{-1} is attributed to the tetrahedral metal–oxygen $(M\text{–}O)_{tet}$ bonds and the peak around 452 cm^{-1} corresponds to vibration of octahedral metal–oxygen $(M\text{–}O)_{oct}$ bonds [15]. The presence of these peaks confirmed the formation of metal–oxygen bands in the tetrahedral and octahedral sublattices of the $MnFe_2O_4$ nanoparticles.

Fig. 3 shows FESEM micrographs of the samples. From this figure, the P0 sample consists of large particles with average diameter of ~50 nm. It seems that the large particles are aggregates of several smaller particles which was confirmed by TEM image. For P10 and P20 samples, there is no clear trace of ferrite particles in the FESEM images probably due to high wax concentration in these samples. TEM image of P0 sample is shown in Fig. 4a. Particles with size of about 6 nm is seen in the TEM image, which is in good accordance with the crystallite size obtained using Scherrer's